

useful structural and dynamic information about Cd^{2+} in large molecules.

Acknowledgment. D.M.K. acknowledges support from donors of the Petroleum Research Fund, administered by the American Chemical Society. S.L. acknowledges support by a "Postgraduate Scholarship" from the Natural Sciences and Engineering Research

Council of Canada. We thank Dr. Bruce Parkinson for donating the sample of CdS and James Richardson for determining the unit cell parameters of $[\text{Cd}_{10}(\text{SCH}_2\text{CH}_2\text{OH})_{16}(\text{ClO}_4)_4]$. The Ames Laboratory is operated for the U.S. Department of Energy by Iowa State University under Contract No. W-7405-Eng-82. This research was supported by the Assistant Secretary for Energy Research, Office of Energy Sciences, WPAS-KC-03-02-01.

Analysis of Field-Dependent Relaxation Data and Hyperfine Shifts of Cytochrome *c'* from *Rhodospirillum rubrum* in Terms of the High-Spin Iron Ligation States

Gerd N. La Mar,* J. Timothy Jackson, and R. G. Bartsch†

Contribution from the Departments of Chemistry, University of California, Davis, California, 95616, and University of California, San Diego, La Jolla, California 92093.
Received December 18, 1980

Abstract: The pH and field dependence of the paramagnetic line widths of the heme methyl resonances of cytochrome *c'* from *Rhodospirillum rubrum* (strain 1 DTCC) have been analyzed for the purpose of extracting information on the ligation states of the protein in both its oxidized and its reduced high spin forms. The methyl line widths in all protein forms were found to exhibit substantial quadratic field dependence consistent with significant contribution from Curie spin relaxation. For ferricytochrome *c'*, the field-independent contribution to the methyl line width differed substantially between the acid-to-neutral pH form (I) and form II, stable in the pH range 9–11. Comparison of the calculated electron relaxation times indicates that form I has a weaker axial ligand field than either form II or aquometmyoglobin, which favors a five-coordinate I and a six-coordinate II. The appearance of two new resonances in the far downfield region upon converting I → II, without the apparent loss of any hyperfine shifted signals from I, confirms the coordination of a sixth ligand in II. Qualitative comparisons of the line widths of these two new signals to those of the heme methyls support an acidic residue as the sixth ligand. The detection of the characteristic exchangeable proton resonance of an axial imidazole and the importance of Curie spin relaxation in ferrocycytochrome *c'* confirm its high-spin five-coordinated structure.

Cytochromes *c'* are a group of primarily dimeric hemoproteins found in a variety of photosynthetic and denitrifying bacteria. Although their precise function remains to be established, cytochromes *c'* probably act as electron-transport proteins.¹ Initial spectroscopic^{2,3} and susceptibility^{4,5} studies revealed these proteins to be essentially high spin in both their redox states, in contrast to the more usual low-spin mitochondrial or bacterial cytochromes *c*. They share with the latter class of proteins⁶ the invariant peptide fragment, Cys-X-X-Cys-His (Figure 1A), toward the C-terminal end of the molecules at residues approximately 116–120. While this fragment provides both the covalent links to the heme and the axial histidyl imidazole^{7,8} the nature of the sixth ligand, at least in the ferric state, remains in question in all three of the forms the protein adopts in different pH ranges. A single-crystal X-ray diffraction study⁹ of the dimeric cytochrome *c'* from *Rhodospirillum molischianum* has confirmed an axial histidine for each of the equivalent ferric hemes, but the resolution is not yet sufficiently high to permit unambiguous conclusions as to the presence of a coordinated water in the neutral pH form of the protein.

For the ferrous form in the neutral pH range, optical, susceptibility, near-infrared MCD, and resonance Raman data all agree on a five-coordinated form very similar to deoxymyoglobin.^{2-5,10-13} The ferric form adopts three spectroscopically distinct forms designated I (pH 5–9), II (pH 9–11), and III (pH ≥ 12).² Early ESR¹⁰ and resonance Raman¹¹ work revised the original high-spin formulation for I at low pH, instead suggesting the existence of a quantum mechanical mixed-spin, $S = 3/2, 5/2$, state. More recent Mössbauer¹² and near-IR MCD¹³ data, however, favor the initial high-spin ground state. Although resonance Raman spectra were originally interpreted¹⁴ in terms

of a five-coordinate species for I, subsequent revision has suggested¹⁵ a six-coordinate species with an oxygen-bound ligand that is lost upon converting to II in the weakly alkaline region. In contrast, the increase in energy of near-IR bands on converting from I → II has led to the proposal that a five-coordinate species

- (1) Bartsch, R. G. In "The Photosynthetic Bacteria"; Clayton, R. K., Siström, W. R., Eds.; Plenum Press: New York, 1978; 249–279.
- (2) Horio, T.; Kamen, M. D. *Biochim. Biophys. Acta* **1961**, *48*, 266–286.
- (3) Imai, Y.; Imai, K.; Sato, R.; Horio, T. *J. Biochem. (Tokyo)* **1969**, *65*, 225–237.
- (4) Kamen, M. D.; Kakuno, T.; Bartsch, R. G.; Hannon, S. *Proc. Nat. Acad. Sci. U.S.A.* **1973**, *70*, 1851–1854.
- (5) Moss, T. H.; Bearden, A. J.; Bartsch, R. G.; Cusanovich, M. A. *Biochemistry* **1968**, *7*, 1583–1590.
- (6) Ehrenberg, A.; Kamen, M. D. *Biochim. Biophys. Acta* **1965**, *102*, 333–340.
- (7) Tasaki, A.; Otsuka, J.; Kotani, M. *Biochim. Biophys. Acta* **1967**, *140*, 284–290.
- (8) Salemme, F. R. *Annu. Rev. Biochem.* **1977**, *46*, 299–329.
- (9) Meyer, T. E.; Ambler, R. P.; Bartsch, R. G.; Kamen, M. D. *J. Biol. Chem.* **1975**, *250*, 8416–8421.
- (10) Ambler, R. P.; Daniel, M.; Meyer, T. E.; Bartsch, R. G.; Kamen, M. D. *Biochem. J.* **1979**, *177*, 819–823.
- (11) Weber, P. C.; Bartsch, R. G.; Cusanovich, M. A.; Hamlin, R. C.; Howard, A.; Jordan, S. R.; Kamen, M. D.; Meyer, T. E.; Weatherford, D. W.; Xuong, Ng. H.; Salemme, F. R. *Nature (London)* **1980**, *286*, 302–304.
- (12) Maltempo, M. M.; Moss, T. H.; Cusanovich, M. A. *Biochim. Biophys. Acta* **1974**, *342*, 290–305.
- (13) Streckas, T. C.; Spiro, T. G. *Biochim. Biophys. Acta* **1974**, *351*, 237–245.
- (14) Emptage, M. H.; Zimmermann, R.; Que, Jr., L.; Münck, E.; Hamilton, W. D.; Orme-Johnson, W. H. *Biochim. Biophys. Acta* **1977**, *495*, 12–23.
- (15) Rawlings, J.; Stephens, P. J.; Jafie, L. A.; Kamen, M. D. *Biochemistry* **1977**, *16*, 1725–1729.
- (16) Kitagawa, T.; Ozaki, Y.; Kyogoku, Y.; Horio, T. *Biochim. Biophys. Acta* **1977**, *493*, 1–11.
- (17) Teraoka, J.; Kitagawa, T. *J. Phys. Chem.* **1980**, *84*, 1928–1935.

* University of California, San Diego.

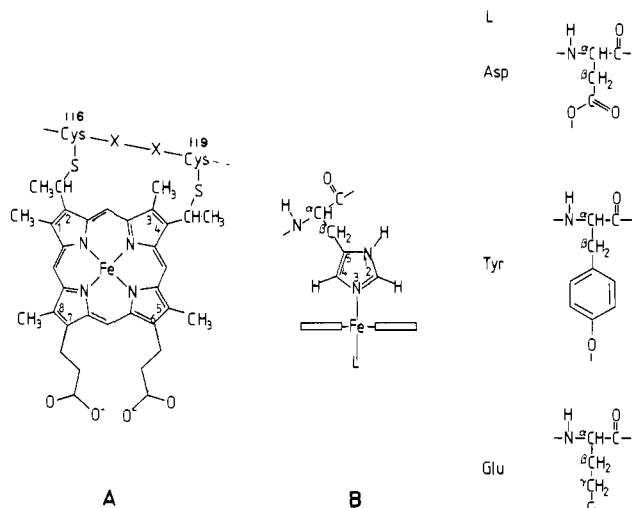


Figure 1. Structure of heme *c* (A) with ligated histidine and possible sixth ligand (B) (for discussion see text).

adds an oxygen-bound ligand.¹³ All data agree that the species in strongly alkaline solution (III) is low spin, with presumably a bound lysine.¹⁰⁻¹⁴

A recent proton NMR study¹⁶ of both ferro- and ferricytochrome *c'* from *Rhodospirillum rubrum* has demonstrated that the hyperfine shifts in the ferric form reflect two pK's of 5.8 and 8.7; the protein denatures above pH 11.¹⁶ The former pK, undetected by other spectroscopy, was proposed to arise from titration of the second, nonfunctional histidine within I; the latter pK corresponds to the conversion I \rightleftharpoons II and exhibited large shift changes indicative of rapid averaging over the two environments on the NMR time scale. It was suggested that I is five-coordinate, with II involving the additional coordination of a carboxylate, possibly at position 122.

While the proton NMR hyperfine shifts for cytochrome *c'*, as well as for other paramagnetic hemoproteins,¹⁶⁻¹⁹ have been demonstrated to be sensitive indicators of changes in protein conformation, the concomitant paramagnetic relaxation data²⁰ have received considerably less attention as probes for changes in the state of the heme in a given oxidation/spin state. High-spin ferric and ferrous hemoproteins present particularly useful subjects for such relaxation studies, since the electron spin relaxation,^{20,21} and hence the proton line width, is controlled by the magnitude of the zero-field splitting of the ground state, which in turn is a sensitive indicator of the strength of the effective axial ligand field.^{22,23}

We present here the results of a study of the field and pH dependence of the proton NMR line widths of the hyperfine shifted resonances of both ferrous and ferric cytochrome *c'* from *Rhodospirillum rubrum* which confirm a pH-independent five-coordinate ferrous protein and support a five-coordinate iron(III) for I which adds a glutamic acid residue on converting to II.

Principles

Paramagnetic relaxation,^{20,24,25} in terms of the proton line width (δ), in a high-spin, $S = 5/2$, ferric system at high magnetic field, B_0 , can be written as the sum of three terms, $\delta = \delta_S(\text{dip}) + \delta_X(\text{dip}) + \delta_A(\text{scalar})$, with

$$\pi\delta_S = (7/15)\gamma^2\mu_S^2r^{-6}T_{1e} \quad (1)$$

$$\pi\delta_X = [4\gamma^2\mu_S^4r^{-6}B_0^2/(45k^2T^2)]\tau_r \quad (2)$$

$$\pi\delta_A = (\mu_S^2/3g^2\beta^2)(A/\hbar)^2T_{1e} \quad (3)$$

where δ_S represents the normal dipolar relaxation by the instantaneous spin^{20,26} S , δ_X is due to dipolar relaxation by the novel Curie spin mechanism^{24,25,27} involving the time-averaged S , and δ_A results from modulation of the scalar coupling²⁰ constant which gives rise to the contact shift; T_{1e} is the electron spin relaxation time, τ_r the correlation time for rotational diffusion of the whole protein, μ_S = electronic magnetic moment, B_0 the applied field, r the iron-proton distance, and A/\hbar the Fermi scalar coupling constant.²⁶ For all model complexes studied²⁸ and most iron proteins,^{19,26} the δ_S term dominates, with δ_A sometimes making important contributions. However, for sizable proteins (large τ_r) with large magnetic moments, μ_S , large applied fields, B_0 , and short T_{1e} 's, the second term can easily dominate the overall relaxation.^{24,25} Such has been found to be the case in high-spin ferrous hemoglobin.²⁷

Factoring the various contributions prior to analysis of the relaxation is important for at least two applications. Comparison of relative values of δ_S or δ_X for nonequivalent protons in the same molecule directly yields distance estimates via

$$\delta_S(i)/\delta_S(j) = \delta_X(i)/\delta_X(j) = r_i^{-6}/r_j^{-6} \quad (4)$$

Since δ_X depends on B_0^2 , it can always be separated from δ_S and δ_A . On the other hand, unless the relative values of r^{-6} and A/\hbar are known, δ_S and δ_A cannot be readily separated. Secondly, a comparison of T_{1e} 's for two proteins or for two forms of the same protein requires comparison of the field-independent terms δ_S and/or δ_A .

Relative values of T_{1e} 's yield useful information on the relative zero-field splitting constant, D , in high-spin iron systems.^{20,21} The paramagnetic relaxation of high-spin ferric models has already been shown²⁸ to be dominated by modulation of the zero-field splittings, for which the relationship

$$T_{1e} \propto D^{-2} \quad (5)$$

holds. Such a trend was established for a series of model compounds^{21,28} and is indicated to be valid for high-spin ferric myoglobin, for example, where replacement of H_2O with F^- yields to significant broadening of all lines²⁹ consistent with the dramatic decrease²³ in the value of D . Changes in D for a set of isostructural chromophores can be readily related to changes in the effective axial ligand field strength.^{21,22} In the present case,¹² as for myoglobin,²³ D is positive, dictating that a reduction in the magnitude of D reflects an increase in the effective axial ligand field strength.

Experimental Section

Cytochrome *c'* from *Rhodospirillum rubrum* was isolated and purified by previously published methods.³⁰ Solutions of 2 mM concentration of the ferric form of cytochrome *c'*, cyto"*c'*", were prepared by dissolving

(16) Emptage, M. H.; Xavier, A. V.; Wood, J. M.; Alsaadi, M.; Moore, G. R.; Pitt, R. C.; Williams, R. J. P.; Ambler, R. P.; Bartsch, R. G. *Biochemistry* **1980**, *19*, 58-64.

(17) Morrow, J. S.; Gurd, F. R. N. *CRC Crit. Rev. Biochem.* **1975**, *3*, 221-287.

(18) La Mar, G. N. In "Biological Applications of Magnetic Resonance"; Shulman, R. G., Ed.; Academic Press: New York, 1979; pp 305-343.

(19) La Mar, G. N.; Budd, D. L.; Smith, K. M.; Langry, K. C. *J. Am. Chem. Soc.* **1980**, *102*, 1822-1827.

(20) Swift, T. J. In "NMR of Paramagnetic Molecules"; La Mar, G. N., Horrocks, W. D., Jr., Holm, R. H., Eds.; Academic Press: New York, 1973; pp 53-83.

(21) La Mar, G. N.; Walker, F. A. *J. Am. Chem. Soc.* **1973**, *95*, 6950-6956.

(22) Ballhausen, C. J. "Introduction to Ligand Field Theory"; McGraw-Hill: New York, 1962; Chapter 6.

(23) Brackett, G. C.; Richards, P. L.; Caughey, W. S. *J. Chem. Phys.* **1971**, *54*, 4383-4401.

(24) Gueron, M. *J. Magn. Reson.* **1975**, *19*, 58-66.

(25) Vega, A. J.; Fiat, D. *Mol. Phys.* **1976**, *31*, 347-355.

(26) The equations for $\delta_S(\text{dip})$ and $\delta_A(\text{scalar})$ are given for the limit $\omega_S^2 T_{1e}^2 \gg 1$, as is the likely case here; at 360 MHz $\omega_S = 1.49 \times 10^{12} \text{ s}^{-1}$ and the T_{1e} determined from field-independent line width and known distance yields $T_{1e} \geq 7 \times 10^{-12} \text{ s}$ for all cases of interest here.

(27) Johnson, M. E.; Fung, L. W.-M.; Ho, C. *J. Am. Chem. Soc.* **1977**, *99*, 1245-1250.

(28) La Mar, G. N.; Walker-Jensen, F. A. In "The Porphyrins"; Dolphin, D., Ed.; Academic Press: New York, 1979; Vol. IV, pp 61-157.

(29) Morishima, I.; Neya, S.; Ogawa, S.; Yonezawa, T. *FEBS Lett.* **1977**, *83*, 148-150.

(30) Bartsch, R. G. *Methods Enzymol.* **1971**, *23*, 344-363.

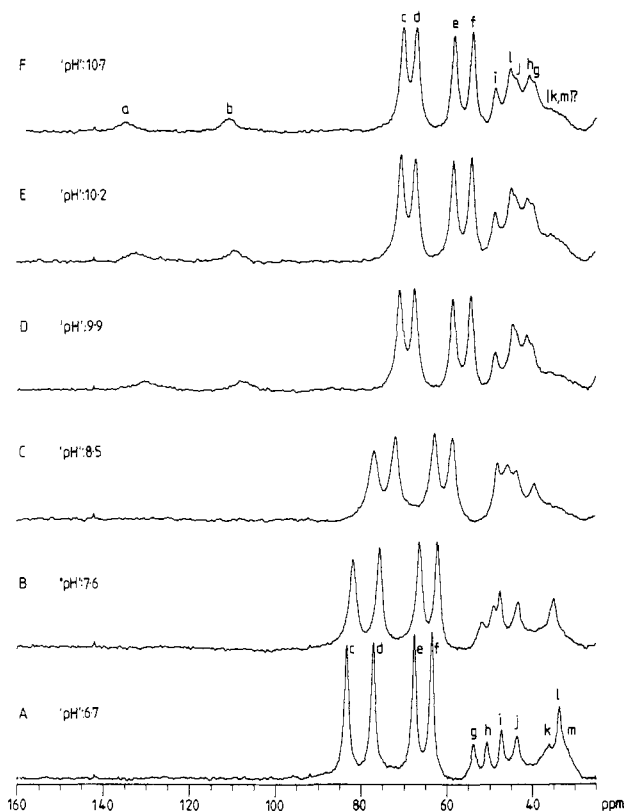


Figure 2. 360-MHz ^1H NMR spectra of the region 25–160 ppm downfield from DSS for 2 mM *R. rubrum* ferricytochrome *c'* in D_2O at 25 $^\circ\text{C}$ and at “pH” 6.7 (A); 7.6 (B); 8.5 (C); 9.9 (D); 10.2 (E); 10.7 (F).

the protein in 99.8% $^2\text{H}_2\text{O}$ (or 90% H_2O :10% $^2\text{H}_2\text{O}$) and centrifuging to remove any undissolved solids. The “pH” was adjusted by the addition of small aliquots of 0.1 M NaOH (or NaOH) or 0.1 M HCl (or HCl). The reduced form of the protein was prepared by the addition of a minimum quantity of solid sodium dithionite to a solution of the ferric form under an atmosphere of nitrogen.

^1H NMR spectra (100-MHz) were recorded on a JEOL JMN 100 spectrometer operating in the Fourier transform mode. Typical spectra consisted of collecting 150 transients into 8K data points over a 25-kHz bandwidth (20 μs , 90° pulse) and Fourier transforming the data set with the introduction of a line broadening of 30 Hz in order to increase the signal-to-noise ratio. About 60 such transformed data sets were coherently added, while allowing the signal due to residual H_2O to overflow the computer memory. Nicolet NT-200 and NT-360 FT spectrometers, both operating with digital quadrature detection, were used for recording 200-MHz and 360-MHz ^1H NMR spectra, respectively. Typical spectra involved the application of a presaturation pulse of 35 ms (450 ms in 90% H_2O) to the residual H_2O signal and collecting 5000 transients into 16K data points for a bandwidth of 300 ppm (10 μs , 90° pulse). Comparison spectra in the absence of, and presence of, the presaturation of the H_2O line for the reduced species were obtained using the “2-1-4” phase-shifted observation pulse of Redfield^{31,32} centered at ca. 84 ppm downfield from 2,2-dimethyl-2-silapentane-5-sulfonate (DSS). The signal-to-noise ratio was increased by exponential multiplication of the free induction decay prior to Fourier transformation; this introduced a line broadening of 20–100 Hz. Line widths were either measured directly from the plotted spectra or determined by computer line-fitting routines (NTCCAP) available on the Nicolet NTC-1180 data systems; account was taken of the artificially induced line broadening. All chemical shifts were indirectly referenced to DSS via the residual H_2O signal. The pH was measured with a Beckman Model 3500 pH meter equipped with an Ingold microcombination electrode; the values are uncorrected for isotope effects and are referred to as “pH”.

Results and Discussion

Ferricytochrome *c'*. Analysis of Line Widths. The 360-MHz proton NMR spectra of *R. rubrum* ferricytochrome *c'* in $^2\text{H}_2\text{O}$

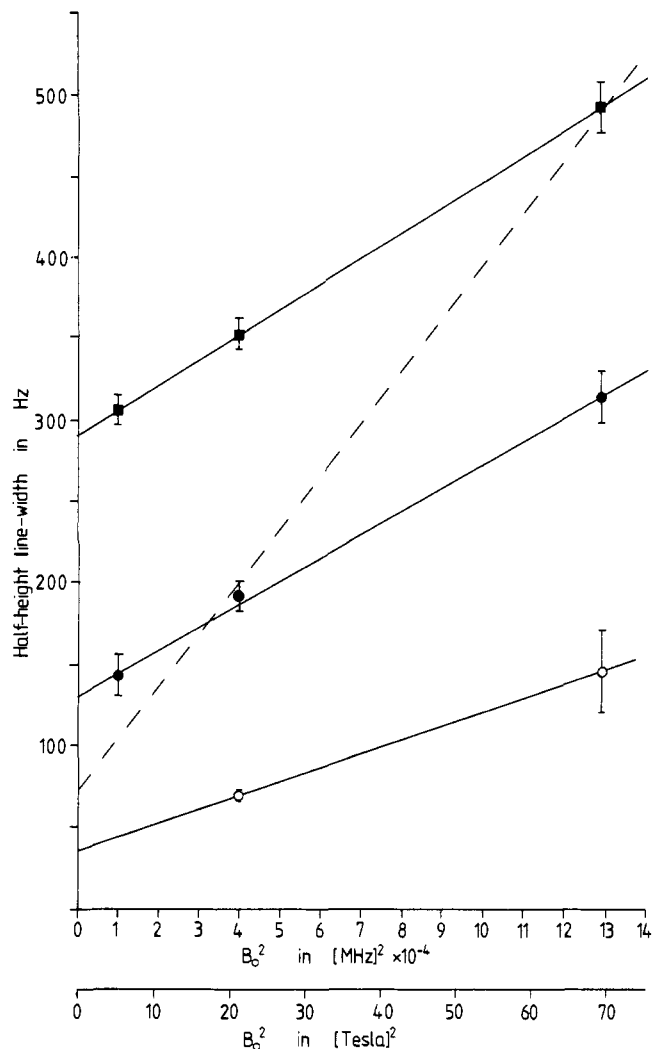


Figure 3. Plot of observed half-height line width vs. the square of the nuclear magnetic resonant frequency for the postulated heme methyl signals in *R. rubrum* ferricytochrome *c'* at “pH” 6.8 (●) and at “pH” 10.5 (■). Also shown is the field dependence of the line widths of the postulated heme methyl signals (○) and the assumed proximal histidyl imidazole 1-H (---) at pH 5.4 in the reduced form of the cytochrome *c'*.

at 25 $^\circ\text{C}$ and various “pH” values are given in Figure 2; no additional lines are resolved in H_2O solution. The peaks resolved in the spectral region 90–25 ppm, labeled c–m (an additional single proton peak, n, is observed¹⁶ at 20 ppm), are the same as those found previously at 270 MHz, except for the improved signal-to-noise ratio. While the line widths of the resolved peaks c–f, presumed to be heme methyls (A in Figure 1), do not vary detectably between “pH” 5 and 7 (I), they do increase markedly upon converting to II, which is the only species present at “pH” 10.7. Plots of the methyl line widths (c–f) as a function of B_0^2 for I (“pH” 6.8) and II (“pH” 10.7) are illustrated in Figure 3. These four peaks have the same line widths within experimental error at each of the two “pH” values. The straight lines in Figure 3 clearly demonstrate that there is a large component of the line width which arises from the Curie spin mechanism^{24,25} for both I and II. Although this mechanism has been previously demonstrated for high spin ferrous hemoproteins,²⁷ ferricytochrome *c'* represents the first ferric hemoprotein exhibiting important contributions from Curie spin relaxation. The field-independent line width is extrapolated as 130 ± 10 Hz for each of the four methyls, c–f, for I of cytochrome *c'*.

In the case of high-spin ferric aquometmyoglobin, essentially field independent line widths of 300 Hz have been reported.¹⁹ The fact that the four methyls all have identical line widths for each protein in spite of exhibiting a range of chemical shifts argues

(31) Redfield, A. G.; Kunz, S. D.; Ralph, E. K. *J. Magn. Reson.* **1975**, *19*, 114–117.

(32) Cutnell, J. D.; La Mar, G. N.; Kong, S. B. *J. Am. Chem. Soc.*, submitted for publication.

against a significant contribution from δ_A (which would introduce a line width contribution quadratic in the size of the contact shift, as observed³³ in some other high-spin proteins). Since we are comparing the heme methyl line widths for protons (heme methyls) which have the same r^{-6} in the two proteins, and using the known magnetic moments³⁴, the ratios of δ_S yield

$$\delta(\text{Mb})/\delta(\text{cyto I}) = [\mu_S^2(\text{Mb})/\mu_S^2(\text{cyto I})]T_{1e}(\text{Mb})/T_{1e}(\text{cyto I}) \quad (6)$$

which yields $T_{1e}(\text{cyto I}) \simeq 0.5 T_{1e}(\text{Mb})$. On the basis of eq 6, therefore, we can conclude that the zero-field splitting constant, D , is significantly larger in ferricytochrome $c'I$ than in aquometmyoglobin³⁵ and that the axial ligand field must be weaker in the former protein. Since both proteins possess the same axial histidyl imidazole, any sixth ligand in cytochrome c' must be much weaker than the H_2O in myoglobin, and hence we favor a five-coordinated structure for ferricytochrome $c'I$. The importance of Curie spin relaxation^{24,25} for the latter protein but not for aquometmyoglobin is due to the longer T_{1e} and shorter τ_r in the latter protein.³⁶

Analysis of the changes in methyl line widths (c-f) on converting I to II proceeds along similar lines. The methyl intercept for II at pH 10.7 in Figure 3 yields 300 Hz, which is essentially the same as that found for metMb(H_2O). Comparing cyto $'''c'II$ to either cyto $'''c'I$ or metMb(H_2O) yield

$$T_{1e}(\text{cyto II})/T_{1e}(\text{cyto I}) \simeq 2.0 \quad (7)$$

$$T_{1e}(\text{cyto II})/T_{1e}(\text{Mb}) \simeq 1.0 \quad (8)$$

Equation 7 shows that cyto $'''c'II$ has a T_{1e} twice as long as I, which is independently confirmed in (8) where we show that T_{1e} 's for metMb(H_2O) and cyto $'''c'II$ are very similar. The slopes of the plots of line width vs. B_0^2 in Figure 3 are given by $[4\gamma^2\mu_S^4r^{-6}/45k^2T_2]\tau_r$. A comparison of the slopes for cyto $'''c'II$ $[(15.5 \pm 2.5) \times 10^{-4}]$ to that for cyto $'''c'I$ $[(14.1 \pm 18.0) \times 10^{-4}]$, yields, assuming identical τ_r ,

$$\text{slope}(\text{cyto}'''c'II)/\text{slope}(\text{cyto}'''c'I) = \mu_S^4(\text{II})/\mu_S^4(\text{I}) \quad (9)$$

The experimentally determined slope ratio is 1.1 ± 4 , while the ratio of known¹⁶ μ_S 's yields 1.43 ± 0.20 . Hence the NMR line widths are consistent with the absence of significant conformational change of the protein which would appreciably influence the rotational correlation time.

The increase in T_{1e} upon converting from I to II dictates a smaller value for D for the alkaline form³⁵ and hence, a stronger axial field. Thus the line width change observed in the I \rightarrow II conversion is consistent with an increase in coordination number to six. However, on the basis of the above arguments, a simple change in the iron-imidazole bonding, without a change in coordination number (possibly induced by a protein conformational change), cannot be eliminated. More definitive support for five- and six-coordinated structures for I and II, respectively, can be derived from detailed reanalysis of the "pH" dependence of the positions of the hyperfine shifted resonances.

Dynamics of the I, II Conformational Equilibrium. Although the interconversion between I and II was reported to be fast on the NMR time scale,¹⁶ analysis of the "pH" dependence of the 360-MHz methyl line widths at 25 °C shows that not only do the line widths differ for pure I and II, but they vary with "pH" so

as to be maximum at $\text{pK} = 8.6$, as also illustrated in Figure 2. The fact that the line width maxima occur at the pK and are largest for the peak undergoing the largest shift change (c) dictates that the excess line width arises from chemical exchange, as given³⁷ by

$$\delta_{\text{obsd}} = f_I\delta_I + f_{II}\delta_{II} + \pi f_I^2 f_{II}^2 (\omega_{II} - \omega_I)^2 (\tau_I + \tau_{II}) \quad (10)$$

where f_i , ω_i , and τ_i are the mole fraction, chemical shift, and lifetimes for $i = I, II$ and δ_I, δ_{II} are the line widths of I and II in the absence of exchange. Analysis of the data in Figure 2 yields $\tau_I = \tau_{II} \sim 2.0 \times 10^{-5}$ s at the pK . Thus all peaks exhibiting a chemical shift difference < 8 kHz at 360 MHz exhibit averaged resonances, while all protons having shift differences between I and II greater than this value must display resolved resonances for each species.

Nature of the Sixth Ligand. Extensive studies of high-spin ferric model compounds²⁸ and some hemoproteins^{18,19} have shown that only the four heme methyls, two 2,4-vinyl H_α 's, and four 6,7-propionic acid H_α 's (A in Figure 1) resonate downfield of 10 ppm from DSS. This permits four methyl signals and six single proton resonances below 10 ppm. Thus two of the eight single-proton resonances g-n (n not shown¹⁶) must arise from the axial histidine,³⁸ since high-spin ferric ions exhibit very small magnetic anisotropy or dipolar shifts.^{18,28} The most likely candidates from the histidine ligand are the diastereotopic $\beta\text{-CH}_2$ (or 5-CH_2) (see B of Figure 1). The pH titrations of six of the narrower single proton resonances, g-j, l, n, have been followed in detail previously¹⁶ at 270 MHz. The shift changes are clearly consistent with rapid interconversion on the NMR time scale. Two of the broader single proton peaks, k, m (A in Figure 2), which are better resolved at 270 MHz, are not clearly resolvable at intermediate "pH" values, probably due to the exchange broadening of these already broad lines. However, k and m appear not to have shifted outside of the broad envelope 25–55 ppm, as evidenced by the broad shoulder near 35 ppm for II at "pH" 10.7 (F in Figure 2), and hence experience appreciable hyperfine shifts in both I and II. Thus the conversion I \rightarrow II does not appear to break the iron-histidine bond.

Direct evidence for the addition of a sixth ligand upon forming II is found in the spectral region 100–150 ppm from DSS for which no resonances have been previously reported.¹⁶ Although this region is featureless at low "pH", a pair of severely broadened resonances begin to appear at "pH" 8.9, move downfield slightly, and sharpen to attain single-proton intensity at "pH" 10.7 with shifts of 111 and 135 ppm. The shift and line width properties of these two peaks, labeled a and b in Figure 2, when considered from the point of view of lowering the "pH" from 10.7, are consistent with the onset of chemical exchange in the NMR slow exchange limit ($\omega_I - \omega_{II} > 11$ kHz). Since these two peaks did not exhibit detectable hyperfine shifts for I, they must resonate in the diamagnetic region, requiring that $\omega_{II} - \omega_I \sim 2.5 \times 10^5$ Hz, which is consistent with the observed slow exchange behavior. At "pH" 10.7, where exchange broadening is insignificant for both a and b, we measure line widths of 1.2 and 1.0 kHz, respectively, at 360 MHz and 25 °C. Thus a new functional group must become coordinated to the iron upon converting I \rightarrow II without loss of the histidine.

The pair of protons probably arise from a diastereotopic methylene group of the sixth appended amino acid, which has been proposed^{13,16} to be an oxygen-donor ligand, such as a carboxylate or tyrosinate. Since the protein remains high spin, the sixth ligand is unlikely to be a strong field ligand such as arginine or lysine. Although the pK for the I \rightleftharpoons II transition is quite distant from normal carboxylates, it is quite possible that the structural change that causes coordination of the sixth ligand is triggered by the deprotonation of some remote as yet unspecified amino acid side chain. Some clues as to the identity of this sixth ligand can also

(33) La Mar, G. N.; de Ropp, J. S.; Smith, K. M.; Langry, K. C. *J. Biol. Chem.* **1980**, *256*, 237–243.

(34) Solution μ_S for ferricytochrome $c'I$ and II have been reported as 5.4 ± 0.1 and $5.9 \pm 0.1 \mu_B$, respectively.¹⁶ μ_S for aquometmyoglobin is $5.9 \mu_B$.

(35) The low-temperature values for D for both proteins have been reported, 9.5 cm^{-1} for aquometmyoglobin²³ and $15\text{--}20 \text{ cm}^{-1}$ for ferricytochrome $c'I$ ¹³ and are consistent with our findings in solution at ambient temperature. D for ferricytochrome $c'II$ was reported¹³ as $8.7 \pm 0.5 \text{ cm}^{-1}$, essentially the same as that of aquometmyoglobin²³.

(36) The field-independent line width of $\sim 300 \text{ Hz}$ ¹⁹ for aquometmyoglobin and the intercepts for the slopes of line width vs. B_0^2 in Figure 3 for ferricytochrome $c'I$ and II yield, using the known iron-heme methyl distance,³³ 6.2 \AA , T_{1e} values of 1.5×10^{-11} , 7.6×10^{-12} , and 1.4×10^{-11} s, respectively.

(37) Pople, J. A.; Schneider, W. G.; Bernstein, H. J. "High Resolution Nuclear Magnetic Resonance"; McGraw-Hill: New York, 1959; Chapter 10.

(38) La Mar, G. N.; de Ropp, J. S.; Smith, K. M.; Langry, K. C. *J. Biol. Chem.* **1980**, *255*, 6646–6652.

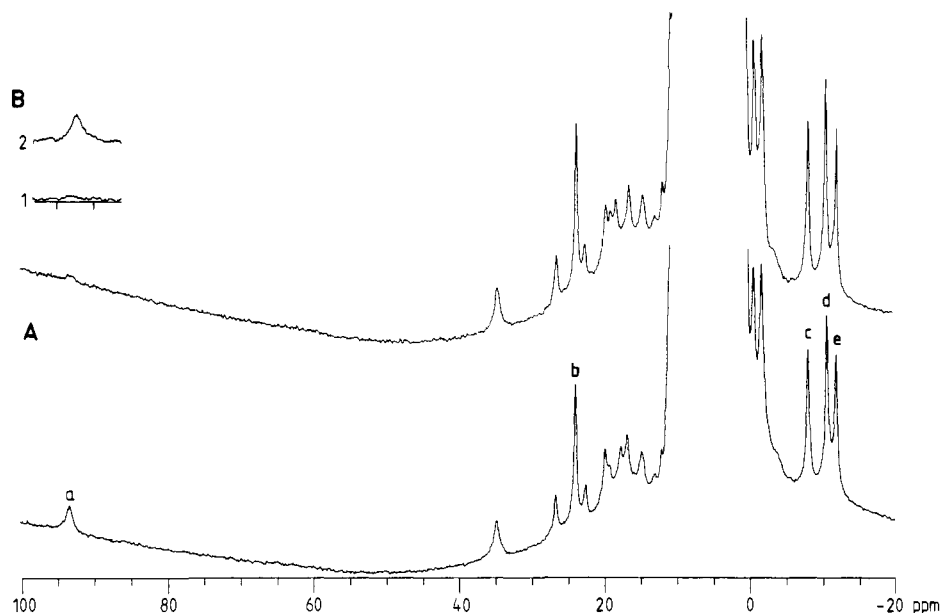


Figure 4. 200-MHz ^1H NMR spectra of the hyperfine shifted regions of 2 mM *R. rubrum* ferrocycytochrome *c'* in H_2O at 25 $^\circ\text{C}$, at pH 5.4 (A) and 6.5 (B). The inset in (B) shows the region from 86–98 ppm, recorded at 360 MHz using the Redfield “2-1-4” observation pulse, with and without presaturation of the H_2O line (1 and 2, respectively).

be derived from the line widths of peaks a, b, and methyls c–f. The line widths for a (1.2 kHz) and b (1.0 kHz) at pH 10.7 lead to δ ratios of $\delta(a)/\delta(\text{CH}_3) = r^{-6}(\text{Fe}-\text{H}_a)/r^{-6}(\text{Fe}-\text{CH}_3) = 2.4$ and $\delta(b)/\delta(\text{CH}_3) = r^{-6}(\text{Fe}-\text{H}_b)/r^{-6}(\text{Fe}-\text{CH}_3) = 2.0$. For a coordinated aspartate, the two β -CH's (B in Figure 1) can be no further than 5.0 Å from the iron, on the basis of reasonable bond length estimates, leading to a predicted ratio $\delta(\beta\text{-CH}_2)/\delta(\text{CH}_3) \geq 4$. Hence a coordinated aspartate can be eliminated from consideration. The meta H (B in Figure 1) signals for coordinated phenoxides in high-spin ferric model compounds and mutant hemoglobins have been located in the region 100 to 150 ppm.³⁹ The computed line width ratios based on estimated distance ratios yield $\delta(\text{Fe}-\text{meta H})/\delta(\text{Fe}-\text{CH}_3) = 0.6\text{--}3.0$, depending on the phenyl rotational position. Although these predicted line widths ratios are consistent with the observed ratios, six-coordinate ferric complexes possessing both imidazole and phenoxide ligands are low spin,⁴⁰ in contrast to the present case; thus a coordinated tyrosinate seems unlikely unless one of the two bonds is considerably weakened.

The most likely candidate seems to be a glutamate ligand, for which the possible β -methylene proton distances to the iron (B in Figure 1) lead to line width ratios in the range $\delta(\beta\text{-CH}_2)/\delta(\text{CH}_3) = 0.8\text{--}14$, depending on the conformation of the carbon backbone, which is consistent with the observed ratios. The absence of data on hyperfine shifts for glutamate coordinated to high-spin iron makes assessment of the shift magnitudes difficult. However, the observation of ~ 140 ppm⁴¹ shifts for the methyl of acetate coordinated to high-spin iron(III) suggests that the observed shifts for a and b may not be unreasonable for the $\beta\text{-CH}_2$ of a coordinated glutamate.

Emptage et al. have suggested¹⁶ an acid residue as the sixth ligand in II based on the frequent occurrence in the amino acid sequences of the cytochromes *c'*, after the Cys-X-X-Cys-His heme-binding fragment, of a triad of residues containing two carboxylic acid residues or one carboxylic and one basic residue, ahead of an invariant aromatic amino acid residue. Our analysis of the NMR spectra supports this hypothesis for *R. rubrum* cytochrome *c'*. However, it is not clear that the distance between the His-120 and Glu-122 in *R. rubrum* cytochrome *c'* is great

enough to permit simultaneous coordination of both the proximal and distal sides of the hemes; therefore it may be necessary to seek the acidic residue elsewhere in the peptide chain. Another possibility is the coordination of an arginyl residue. The available sequence data⁷ include a high degree of conservation toward the N terminal of the protein, in that region of the α helix which traverses the distal side of the heme moiety.⁹ The δ -methylene protons of arginine would be expected to exhibit similar distances from the iron as β -methylene protons of glutamate. Planned NMR studies of cytochromes *c'* possessing different residues may provide more definitive information on the identity of the sixth ligand for state II of cytochrome *c'*.

Ferrocycytochrome *c'*. The 200-MHz proton NMR spectra of ferrocycytochrome *c'* in $^2\text{H}_2\text{O}$ at pH 5.4 and 6.2 are illustrated in Figure 4. The single resolved resonance from an exchangeable proton, a, located at 93 ppm in A, can be assigned to the proximal histidyl imidazole N_1H (B in Figure 1, with no L) found in model compounds⁴² as well as deoxy-myoglobins and -hemoglobins.^{18,39} This resonance disappears at the higher “pH” due to saturation transfer from the water via base-catalyzed proton exchange.³² Peak a can be detected even at “pH” 6.2 by using the Redfield 2-1-4 pulse sequence^{31,32} (as shown in inset of B in Figure 4) which does not excite the H_2O resonance. Peak a is also absent in all $^2\text{H}_2\text{O}$ solutions of the protein.¹⁶ This characteristic imidazole resonance confirms the presence of a five-coordinate high-spin iron(II) with an axial histidine. The remaining nonexchangeable resonances are similar to those reported earlier¹⁶ and do not exhibit marked “pH” dependence in the region 5–10.

The importance of Curie spin relaxation behavior has already been demonstrated in deoxy-myoglobins and -hemoglobins.²⁷ The dependence of the estimated line widths on B_0^2 for the four presumed methyl peaks b–e and the exchangeable peak a are also included in Figure 3. Due to the appreciable overlap experienced by all four methyl signals, the sizable uncertainties, ± 25 Hz, did not permit unambiguous differentiation of the line widths of the peaks b–e at either 200 or 360 MHz. The ratio of the slope of the plots of line width for the peak a to the average value of the four methyls was found to be 3.8 ± 0.8 . From the relationship $\delta(\text{N}_1\text{H})/\delta(\text{CH}_3) = r^{-6}(\text{Fe}-\text{N}_1\text{H})/r^{-6}(\text{Fe}-\text{CH}_3) = 3.8 \pm 0.8$ (eq 1), we obtain the distance ratio $r(\text{Fe}-\text{CH}_3)/r(\text{Fe}-\text{N}_1\text{H}) = 1.25 \pm 0.05$. The usual $\text{Fe}-\text{N}_1\text{H}$ distance for a coordinated imidazole can be estimated as 5.1 Å , leading to $r(\text{Fe}-\text{CH}_3) \sim 6.4 \pm 0.4$

(39) La Mar, G. N.; Nagai, K.; Jue, T.; Budd, D. L.; Gersonde, K.; Sick, H.; Kagimoto, T.; Hayashi, A.; Taketa, F. *Biochem. Biophys. Res. Commun.* **1980**, *96*, 1172–1177.

(40) Ainscough, E. W.; Addison, A. W.; Dolphin, D.; James, B. R. *J. Am. Chem. Soc.* **1978**, *100*, 7585–7591.

(41) La Mar, G. N.; Eaton, G. R.; Holm, R. H.; Walker, F. A. *J. Am. Chem. Soc.* **1973**, *95*, 63–75.

(42) La Mar, G. N.; Budd, D. L.; Goff, H. *Biochem. Biophys. Res. Commun.* **1977**, *77*, 104–110.

Å, which is consistent with all four peaks, b-e, originating from the heme methyls [calculated $\tau(\text{Fe}-\text{CH}_3) \sim 6.2 \text{ \AA}$].

Conclusions

The present NMR study leads to the conclusions that the differences in ferricytochrome *c'* line widths of heme methyl resonances in I and II support a five-coordinate I and a II with a stronger axial ligand field which is consistent with six-coordination. The emergence of two new hyperfine shifted resonances during the I \rightarrow II conversion confirms the six-coordinate nature of II, and qualitative analysis of their line widths favors their origin

in the β -CH₂ of a glutamate ligand. The detection of an exchangeable resonance characteristic of an axial histidyl imidazole N₁H confirms the high-spin five-coordinate nature of ferrocyclochrome *c'*.

Acknowledgment. We are indebted to J. M. Wood and A. V. Xavier for useful discussion and a copy of their manuscript prior to publication. This research was supported by grants from the National Science Foundation, CHE-77-26517 (G.N.L.), PCM 76-81648 (R.G.B.), and the National Institutes of Health, GM 18528-20 and DOE AT 03-78ER-70293 (R.G.B.).

Stereochemistry at Manganese of the Carbon Monoxide Insertion in Pentacarbonylmethylmanganese(I). The Geometry of the Intermediate

Thomas C. Flood,*¹ John E. Jensen, and John A. Statler

Contribution from the Department of Chemistry, University of Southern California, University Park, Los Angeles, California 90007. Received December 5, 1980

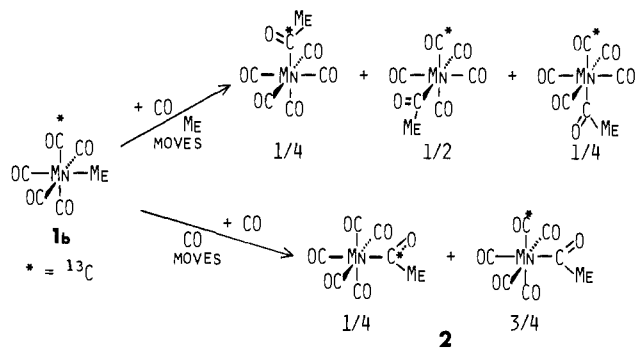
Abstract: The stereochemistry at manganese of the CO insertion into the Me-Mn bond of *cis*-MeMn(CO)₄(¹³CO) has been examined by using ¹³C NMR spectroscopy carried out at -115 °C to give sharp resonances. The insertion was induced by using both ¹²CO and P(OCH₂)₃CMe, each in THF-acetone-*d*₆ and HMPA solvents. The positional ratios of isotopic label in the products are consistent only with methyl migration proceeding through a square-based pyramid with a basal acetyl group in all cases except the ¹²CO-induced insertion in HMPA, in which case the product ratio is that resulting from complete label randomization in the intermediate. From known and estimated kinetic parameters, a ΔG_{298}^\ddagger for isomerization of (MeCO)Mn(CO)₄ of greater than 9 kcal/mol can be inferred.

A complete understanding of the "migratory insertion" of carbon monoxide into metal-carbon σ bonds requires detailed knowledge of a variety of issues, including the stereochemistry at both carbon and the metal, the geometry and stereochemical lability of any intermediates, the role of solvation of transition states and intermediates, and structure-reactivity relationships. Much of this information is currently available for a variety of molecular systems.^{2,3} Nevertheless, reliable stereochemical information regarding the metal center is rather scarce.³

One extensively quoted set of experiments on this last issue dealt with the insertion of Scheme 1.⁴ It was argued that ¹²CO-induced insertion of coordinated CO into the Mn-Me bond of *cis*-MeMn(CO)₄(¹³CO) (**1b**)⁵ would result in one of two site distributions of ¹³CO in (MeCO)Mn(CO)₅ (**2**), depending on whether CO moves to Me or Me moves to CO. In the former case, only *cis* terminal CO would contain label, and in the latter case the *cis/trans* ¹³CO label ratio would be 2/1. A ratio of 2/1 was reported on the basis of IR ¹³CO stretching intensities.⁴

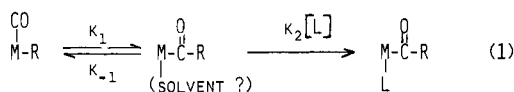
Other studies concerning the stereochemistry at the metal of CO insertion have appeared, including octahedral species such as PhCH₂CH₂RhCl₂(CO)(PPh₃)₂,⁶ EtIrCl₂(CO)₂(AsMe₂Ph),⁷ and MeFeX(CO)₂(PMe₃)₂ (X = I or Me),⁸ square-planar species such

Scheme I



as PhPtCl(CO)(PMePh₂),⁹ and pseudooctahedral (or pseudotetrahedral) species such as η^5 -C₅H₅Fe(CO)(PR₃)R.¹⁰⁻¹² These exhibit a variety of stereochemical paths including apparent CO migration to the alkyl site, apparent alkyl migration to the CO site, and more complicated geometrical reorganization not consistent with either simple CO or R migration.

Kinetics studies of coordinatively saturated complexes are consistent with the predominance of the path shown in eq 1.²



(1) Alfred, P. Sloan Foundation Fellow, 1977-1981.

(2) (a) Wojcicki, A. *Adv. Organomet. Chem.* **1973**, *11*, 87. (b) Calderazzo, F. *Angew. Chem., Int. Ed. Engl.* **1977**, *16*, 299.

(3) Flood, T. C. *Top. Stereochem.* **1980**, *12*, 37.

(4) Noack, K.; Calderazzo, F. *J. Organomet. Chem.* **1967**, *10*, 101.

(5) Nomenclature and structures in this paper are designated as follows: **1** = MeMn(CO)₅, ¹³C label unspecified; **1a** = randomly labeled MeMn(CO)₄(¹³CO); **1b** = *cis*-MeMn(CO)₄(¹³CO); **2** = (MeCO)Mn(CO)₅, ¹³C label unspecified; **2a** = (MeCO)Mn(CO)₄(¹³CO), randomly labelled; mtpb = P-(OCH₂)₃CMe = 4-methyl-2,6,7-trioxo-1-phosphabicyclo[2.2.2]octane; **4** = *cis*-(MeCO)Mn(mtpb)(CO)₄, ¹³C label unspecified; **4a** = *cis*-(MeCO)Mn(mtpb)(CO)₃(¹³CO), randomly labelled.

(6) Slack, D. A.; Egglestone, D. L.; Baird, M. C. *J. Organomet. Chem.* **1978**, *146*, 71. Egglestone, D. L.; Baird, M. C.; Lock, J. C.; Turner, G. J. *Chem. Soc., Dalton Trans.* **1977**, 1576.

(7) Glyde, R. W.; Mawby, R. J. *Inorg. Chim. Acta* **1971**, *5*, 317.

(8) Pankowski, M.; Bigorgne, M. *J. Organomet. Chem.* **1971**, *30*, 227. Pankowski, M.; Bigorgne, M. "Abstracts", The 8th International Conference on Organometallic Chemistry, Kyoto, Japan, 1977.

(9) Anderson, G. K.; Cross, R. J. *J. Chem. Soc., Dalton Trans.* **1979**, 1246.

(10) Attig, T. G.; Wojcicki, A. *J. Organomet. Chem.* **1974**, *82*, 397.

Reich-Rohwig, P.; Wojcicki, A. *Inorg. Chem.* **1974**, *13*, 2457.

(11) Davison, A.; Martinez, N. *J. Organomet. Chem.* **1974**, *74*, C17.

(12) Flood, T. C.; Campbell, K. D.; Downs, H. H.; Statler, J. A.; to be submitted for publication.